

Comparison of strong-coupling theories for a two-dimensional Fermi gas

Brendan C. Mulkerin, Kristian Fenech, Paul Dyke, Chris J. Vale, Xia-Ji Liu, and Hui Hu
Centre for Quantum and Optical Science, Swinburne University of Technology, Melbourne 3122, Australia.
 (Dated: February 16, 2016)

Understanding the formation of Cooper pairs and the resulting thermodynamic properties of low-dimensional Fermi gases is an important area of research, which may help build our understanding of other low-dimensional systems such as high temperature superconductors. In lower dimensions quantum fluctuations are expected to play an increasingly important role and the reliability of strong-coupling theories becomes questionable. Here, we present a comparison of recent thermodynamic measurements and theoretical predictions from different many-body T -matrix theories for a two-dimensional strongly interacting Fermi gas in the normal state. We find that the fully self-consistent T -matrix theory provides the best description of the experimental data over a wide range of temperatures and interatomic interactions.

PACS numbers: 05.30.Fk, 67.85.-d, 03.75.Hh

The understanding of pairing of fermions in strongly interacting two-dimensional (2D) Fermi gases is of great interest to condensed matter physics, where the pairing mechanism in high-temperature superconductors remains elusive [1]. In order to theoretically understand these systems new approaches are required to treat strong interactions as one encounters a “strongly correlated” regime.

The main theoretical difficulty in describing strongly interacting systems is the absence of any small-coupling parameter, which is crucial for truncating perturbative approaches. Due to large quantum fluctuations, mean-field theories do not describe the strongly correlated Fermi gas away from $T = 0$ [2, 3], where correlations beyond the single-particle picture play an important role. There are numerous efforts to develop strong-coupling perturbation theories in both two and three dimensions, notably many-body T -matrix fluctuation theories [4–7], however, the accuracy of such methods is not well understood. Sophisticated quantum Monte Carlo (QMC) simulations have been developed in solving strongly coupled systems, such as diffusion Monte Carlo [8], auxiliary field Monte Carlo [9], lattice Monte Carlo [10], and diagrammatic quantum Monte Carlo [11], however, these approaches also have difficulty evaluating the equation of state. The virial expansion has also been studied in harmonically trapped [12] and homogeneous systems [13], giving exact results in the high-temperature limit.

Recent developments in the experimental realization of two-dimensional ultracold Fermi gases with a tunable interaction through Feshbach resonances, densities, and temperatures provide a unique opportunity to understand and benchmark strong-coupling theories for the two-dimensional BEC-BCS crossover [14–16] and the Berezinskii-Kosterlitz-Thouless (BKT) transition [17]. In these experiments it is possible to extract the density versus chemical potential at a fixed interaction directly from the measured density profile in the trap [18], allowing a direct comparison between theoretical and experimental results. Pairing and superfluidity have been studied for two-dimensional ultracold gases [19], where

the formation of pairs above the superfluid transition T_c , the pseudogap, was examined. The formation of pairs above T_c is a precursor to superfluidity and is important in understanding the BKT transition. In two dimensions the pseudogap regime is expected to be more pronounced than in three-dimensional systems due to the increasingly important quantum fluctuations in low-dimensions [20].

In this paper we draw upon recent experimental data as a benchmark and present a direct comparison of several T -matrix theories as has been performed in 3D [21]. Examining the thermodynamic properties of the density equation of state, pressure equation of state, and compressibility, we show that the fully self-consistent theory successfully describes a 2D Fermi gas over a broad range of temperatures and interaction strengths. We compute the spectral function of the 2D Fermi gas for a fixed interaction strength and temperature currently available to experiment and compare the onset of a pseudogap from the T -matrix theories. This contrasts with the 3D case where the strong-coupling theories disagree over the existence of a pseudogap [22].

The theoretical models compared in this paper are three T -matrix approximations, described briefly here, and for a more detailed description we refer to Refs. [2, 21, 23]. The T -matrix theories involve a partial summation of the infinite set of ladder diagrams, which are generally accepted as the most important contribution in strongly interacting systems. We wish to study the properties of the normal state of a 2D system, i.e., above T_c , where we will set $\hbar = 1$, $k_B = 1$, the mass $2M = 1$, and keep dimensionful variables where instructive. The dressed Green’s function is given by Dyson’s equation,

$$G^{-1}(\mathbf{k}, i\omega) = G_0^{-1}(\mathbf{k}, i\omega) - \Sigma(\mathbf{k}, i\omega), \quad (1)$$

where $\omega = (2m+1)\pi/\beta$ for integer m , $\beta = 1/T$, $\Sigma(\mathbf{k}, i\omega)$ is the self-energy, and the free Green’s function is given by $G_0(\mathbf{k}, i\omega)^{-1} = (i\omega - \varepsilon_{\mathbf{k}} + \mu)$ with $\varepsilon_{\mathbf{k}} = \mathbf{k}^2/(2M)$. The self-energy is given in real space as

$$\Sigma(\mathbf{x}, \tau) = G(-\mathbf{x}, -\tau)\Gamma(\mathbf{x}, \tau), \quad (2)$$

where the regularized vertex function is given through the Bethe-Salpeter equations

$$\Gamma(\mathbf{K}, i\Omega) = \frac{1}{g_0^{-1}(\Lambda) + \chi(\mathbf{K}, i\Omega)}. \quad (3)$$

Here, $\Omega = 2n\pi/\beta$ are the bosonic Matsubara frequencies for integer n , and the pair propagator is given as

$$\chi(\mathbf{K}, i\Omega) = \int \frac{d\mathbf{k}}{(2\pi)^2} \frac{1}{\beta} \sum_{\omega} G(\mathbf{K} - \mathbf{k}, i\Omega - i\omega) G(\mathbf{k}, i\omega). \quad (4)$$

The coupling term $g_0^{-1}(\Lambda)$ is expressed in terms of the physical binding energy, $\varepsilon_B = \hbar^2/(Ma_{2D}^2)$, which is always present in a 2D Fermi gas [24], and a_{2D} is the s -wave scattering length in 2D,

$$g_0^{-1}(\Lambda) = - \int^{\Lambda} \frac{d\mathbf{k}}{(2\pi)^2} \frac{1}{2\varepsilon_{\mathbf{k}} + \varepsilon_B}. \quad (5)$$

Equations (1)–(4), with the regularized two-body interaction, constitute a self-consistent set of coupled integral equations which we solve on a logarithmic grid until convergence is reached. We solve the set of integral equations for a fixed temperature $T > T_c$ and fixed coupling constant $\eta = -1/2 \ln(\varepsilon_B/2E_F) = \ln(k_F a_{2D})$, where the Fermi energy is given by $E_F = k_F^2/2M$ and k_F is the Fermi momentum. Here, T_c is defined by the divergence of the T matrix, the Thouless criterion, $\Gamma^{-1}(\mathbf{q} = 0, \Omega = 0)|_{T=T_c} = 0$. In two dimensions the T -matrix approximation does not recover the BKT transition and the transition temperature is found to be $T_c = 0$, thus we restrict ourselves to an analysis away from the superfluid transition [2]. The chemical potential μ is a free parameter and is fixed by the number equation $n = -2G(\mathbf{x} = 0, \tau = 0^-)$. As in 3D we need to calculate the Fourier transforms efficiently and precisely, carefully considering the singular behavior of the functions $G(\mathbf{x}, \tau)$, $\Gamma(\mathbf{x}, \tau)$, and $\Sigma(\mathbf{x}, \tau)$ and their logarithmic divergences.

From the general self-consistent set of equations it is possible to choose the different T -matrix schemes based upon the choice of interacting and free Green's functions. Firstly, we have the simplest method, the NSR theory, which was originally used to calculate the thermodynamic potential by Nozières and Schmitt-Rink for the BEC-BCS crossover [25]. This theory was extended to two dimensions [26] and is equivalent to calculating a truncated self-energy within the Dyson expansion [27], $G = G_0 + G_0 \Sigma G_0$. The NSR theory can be extended to include all repeated scatterings by summing the full series in the Dyson equation and has been extensively studied in the literature [6], in this work we will only consider the initial truncated case.

The second T -matrix theory considered is the GG_0 theory, where G is an interacting or dressed Green's function. This elevated Green's function must be calculated self-consistently, adding considerable time to the com-

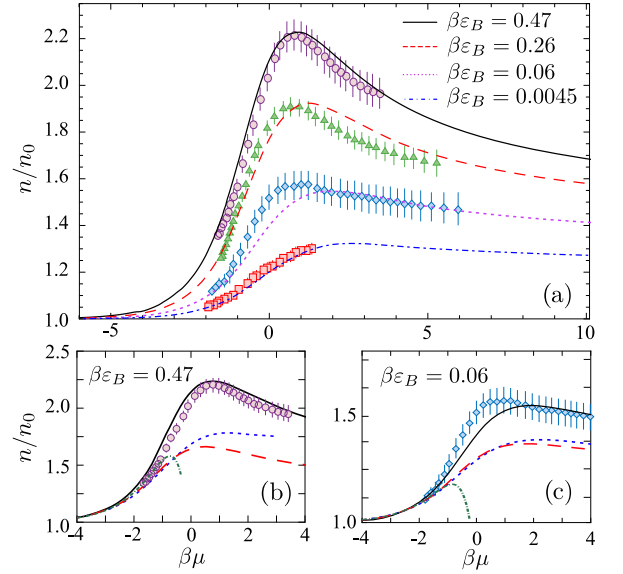


FIG. 1. (Color online) (a) The density equation of state, n/n_0 normalized by an ideal system at the same temperature for the GG theory and experimental results at interaction strengths $\beta\varepsilon_B = 0.47$ (black solid and purple circles), $\beta\varepsilon_B = 0.26$ (red dashed and green triangles), $\beta\varepsilon_B = 0.06$ (purple dotted and blue diamonds) and $\beta\varepsilon_B = 0.0045$ (blue dotted-dashed and red squares). Figures (b) and (c) show a comparison of the three T -matrix theories GG (black solid), GG_0 (red dashed), NSR (blue dotted), third-order virial expansion (green dotted-dashed) and experiment for interaction strengths $\beta\varepsilon_B = 0.47$ and $\beta\varepsilon_B = 0.06$.

putation. One bare G_0 and one self-consistent G enter the vertex equation, while there is a bare G_0 kept in the definition of the fermionic self-energy, Eq. (2).

The final T -matrix theory studied in this paper is the GG theory, where all the single particle Green's function in the vertex and self-energy have been self-consistently calculated. The GG scheme has been studied extensively in the literature for three dimensions and recently in two dimensions and is known as the Luttinger-Ward theory [5]. In three dimensions the GG T matrix yields the best results for calculating the thermodynamic properties of the unitary gas compared to experiment and quantum Monte Carlo [18]. However, the GG theory is far from being exact and has its own shortcomings. For two dimensions in the dilute BEC limit the GG theory is unphysical as it predicts a constant interaction between composite bosons. The non-self-consistent T -matrix theories do not contain this unphysical behavior and better describe the deep BEC limit [28]. Computationally, the non-self-consistent calculations are the simplest to find a converged solution, and it is instructive to compare the T -matrix theories to experiment.

From the converged Green's functions we can find the density equation of state as a function of $\beta\mu$ for a fixed interaction strength $\beta\varepsilon_B$. The density equation of state is given in Fig. 1(a) plotted as a function $\beta\mu$ for in-

$\beta\varepsilon_B$	B (G)	a_{3D} (a_0)	ε_B (Hz)
0.0045	972	-4618.6	4.24
0.06	920	-6354.2	21.00
0.26	880	-10289.6	106.99
0.47	865	-14249.9	222.18

TABLE I. Values of the magnetic fields, scattering length a_{3D} , and binding energy ε_B for the values of $\beta\varepsilon_B$ reported in Fig. 1.

interaction strengths $\beta\varepsilon_B = 0.47$ (black solid and purple circles), $\beta\varepsilon_B = 0.26$ (red dashed and green triangles), $\beta\varepsilon_B = 0.06$ (purple dotted and blue diamonds), and $\beta\varepsilon_B = 0.0045$ (blue dotted-dashed and red squares) for the self-consistent GG theory and experiment. To expose the effects of interactions we have normalized the densities by that of an ideal Fermi gas at the same temperature, $n_0 = 2 \ln[1 + e^{\beta\mu}] / \lambda_T^2$, where $\lambda_T^2 = 2\pi/T$ is the thermal wavelength.

The experimental data shown are taken from Ref. [16], and we briefly describe the experiment here. An isolated 2D Fermi gases of ^6Li atoms is produced in the lowest two spin states $|F = 1/2, m_F = \pm 1/2\rangle$. The cloud is confined to a blue-detuned TEM_{01} mode laser beam that provides tight confinement along z with $\omega_z/2\pi = 5.15$ kHz. Radial confinement is provided by a residual magnetic field curvature when the Feshbach coils are applied and produces a radially symmetric potential with $\omega_r/2\pi = 26$ Hz. The clouds are prepared in the kinematically 2D regime [14] where $N \approx 16000 [= 0.4N_{2D}^{(Id.)}]$, where $N_{2D}^{(Id.)} = (\omega_z/\omega_r)^2$ is the critical atom number] with a temperature range of 20-60 nK.

Imaging of the cloud takes place along z to directly obtain the density $n(x, y)$. Due to the cylindrically symmetric harmonic trap $V_r(x, y)$ we can azimuthally average the images to obtain $n(V_r)$. The $n(V_r)$ data is then used to construct a model independent equation of state for the dimensionless compressibility $\tilde{\kappa} = \kappa/\kappa_0$ and dimensionless pressure $\tilde{p} = P/P_0$ analogous to Refs. [18, 29], where $P_0 = n_0 E_F/2$ and $\kappa_0 = 1/(n_0 E_F)$, at each magnetic field shown in Table I. From these dimensionless values one can obtain the density equation of state, where the reader is referred to Ref. [16] for more of the experimental details. Comparing the GG theory and experimental results, there is good agreement for all the interactions across a broad range of temperatures.

In Figs. 1(b) and 1(c) we compare the density equation of state for an interaction strength of $\beta\varepsilon_B = 0.47$ and $\beta\varepsilon_B = 0.06$, respectively, from each T -matrix theory GG (black solid), GG_0 (blue dotted), NSR (red dashed), third-order virial expansion (green dotted-dashed) and their equivalent experimental results shown with purple circles and blue diamonds. The behavior of the density equation of state for the GG_0 and NSR theories is qualitatively the same, however the results are considerably different from the GG theory and experiment. We

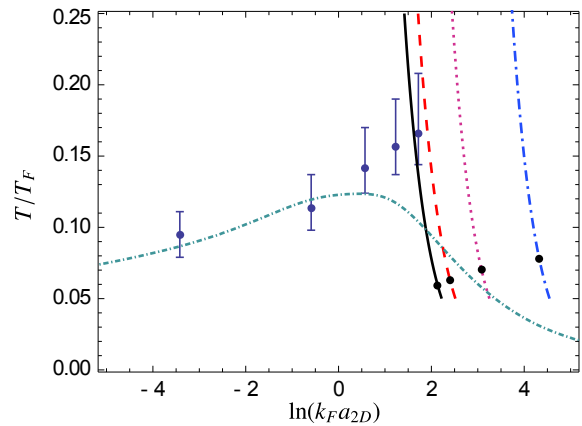


FIG. 2. (Color online) (a) Constant curves of $\beta\varepsilon_B$ given by $\beta\varepsilon_B = 0.47$ (black solid), $\beta\varepsilon_B = 0.26$ (red dashed), $\beta\varepsilon_B = 0.06$ (purple dotted) and $\beta\varepsilon_B = 0.0045$ (blue dotted-dashed). The black dots on each curve are for $\beta\mu = 10$. The experimentally determined BKT transition is given by blue dots with their respective error from Ref. [17], and the theoretical values from Ref. [30] are also given (green short-dotted-dashed).

see that the GG_0 and NSR theories significantly underestimate the density in the strongly interacting regime and in the low temperature, weakly interacting regime. The NSR results in Fig. 1(b) finish at a temperature of $T/T_F \approx 0.19$, where T_F is the Fermi temperature, due to the reliability of the procedure and where the inverse of the vertex function is close to zero [6].

As we go from the high-temperature regime, $\beta\mu = -\infty$ to lower temperatures the gas exhibits a maximum around $\beta\mu \simeq 1$, implying that interactions are strongest at intermediate temperatures. This is understood from the interaction strength $\beta\varepsilon_B$, for a decreasing temperature, T/T_F , corresponds to an increasing interaction $\eta = \ln(k_F a_{2D})$. We see in the low-temperature regime the system is becoming a weakly interacting gas. This behavior can be seen as we plot constant curves of $\beta\varepsilon_B$ for T/T_F as a function of $\ln(k_F a_{2D})$ in Fig. 2, where the curves are given by $\beta\varepsilon_B = 0.47$ (black solid), $\beta\varepsilon_B = 0.26$ (red dashed), $\beta\varepsilon_B = 0.06$ (purple dotted), and $\beta\varepsilon_B = 0.0045$ (blue dotted-dashed). The black dots correspond to a value of $\beta\mu = 10$. For comparison, we have plotted the experimentally determined BKT transition temperature from Ref. [17] and the most recent calculation from Ref. [30], where they have calculated the superfluid transition for the BEC-BCS crossover.

From the density equation of state we can find the pressure through the Gibbs-Duhem relation

$$P(\mu)\lambda_T^4 = \int_{-\infty}^{\beta\mu} n(\beta\mu')\lambda_T^2 d(\beta\mu'). \quad (6)$$

In order to accurately calculate the lower limit of the integration we have used the virial expansion to second order [13] for values of the density as $\beta\mu \rightarrow -\infty$. In

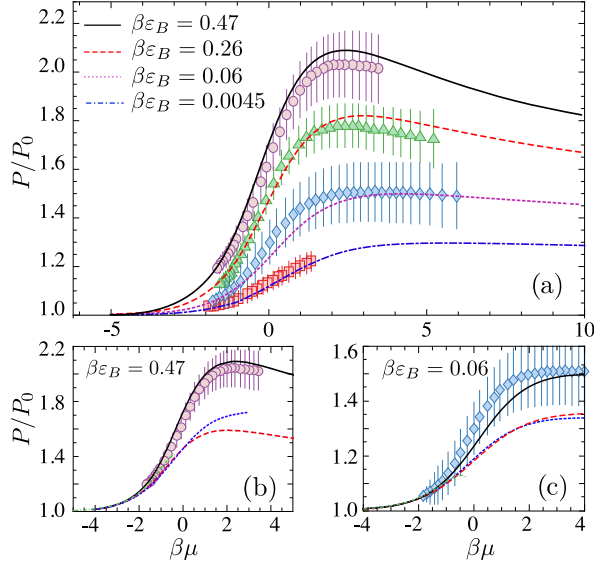


FIG. 3. (Color online) (a) The pressure equation of state P/P_0 normalized by an ideal system at the same temperature for the GG theory and experimental results at interaction strengths $\beta\epsilon_B = 0.47$ (black solid and purple circles), $\beta\epsilon_B = 0.26$ (red dashed and green triangles), $\beta\epsilon_B = 0.06$ (purple dotted and blue diamonds), and $\beta\epsilon_B = 0.0045$ (blue dotted-dashed and red squares). Figures (b) and (c) show a comparison of the three T -matrix theories and experiment GG (black solid), GG_0 (red dashed), and NSR (blue dotted) for interaction strengths $\beta\epsilon_B = 0.47$ and $\beta\epsilon_B = 0.06$.

Fig. 3(a) we plot the normalised pressure as a function of $\beta\mu$ for interaction strengths $\beta\epsilon_B = 0.47$ (black solid), $\beta\epsilon_B = 0.26$ (red dashed), $\beta\epsilon_B = 0.06$ (purple dotted), and $\beta\epsilon_B = 0.0045$ (blue dotted-dashed) for the self-consistent GG theory. We have normalized the pressure by that of an ideal Fermi gas at the same temperature, $P_0\lambda_T^4 = -2\pi\text{Li}_2(-e^{\beta\mu})$ and Li is the polylogarithm. The experimental data in Fig. 3(a) are shown for the same interaction strengths as the theoretical results, $\beta\epsilon_B = 0.47$ (purple circles), $\beta\epsilon_B = 0.26$ (green triangles), $\beta\epsilon_B = 0.06$ (blue diamonds) and $\beta\epsilon_B = 0.0045$ (red squares), allowing for direct comparison. We see that there is good agreement for the four interactions across a broad set of temperatures, showing the maximum in the pressure equation of state near $\beta\mu \simeq 1$ where the interactions are strongest.

In Figs. 3(b) and (c) we plot the pressure equation of state for interaction strengths of $\beta\epsilon_B = 0.47$ and $\beta\epsilon_B = 0.06$, respectively, for the three T -matrix theories GG (black solid), GG_0 (blue dotted), NSR (red dashed), and compare to the experimental results. The GG_0 and NSR underestimate the pressure in the strongly interacting regime compared to the GG theory, as we have seen in the density equation of state.

The compressibility can be found from the density

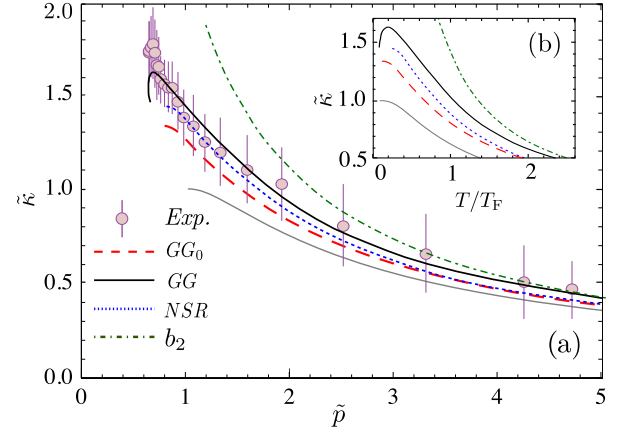


FIG. 4. (Color online) (a) The compressibility $\tilde{\kappa} = \kappa/\kappa_0$ plotted as a function of the pressure $\tilde{p} = P/P_0$ and (b) compressibility as a function of reduced temperature, where $P_0 = n_0 E_F/2$ and $\kappa_0 = 1/(n_0 E_F)$ are the ideal compressibility and pressure at zero temperature and interaction of $\beta\epsilon_B = 0.47$. In each plot we have the T -matrix theories GG (black solid), GG_0 (red dashed), NSR (blue dotted), and experiment (purple circles). For comparison, we plot also the prediction from the second-order virial expansion (green dotted-dashed) and ideal compressibility (gray) as a function of pressure or temperature.

equation of state through the relation

$$\kappa = \frac{\beta}{n^2} \frac{\partial n}{\partial(\beta\mu)} \bigg|_T = \frac{\lambda_T^4}{2\pi} \frac{1}{(n\lambda_T^2)^2} \frac{\partial n\lambda_T^2}{\partial(\beta\mu)} \bigg|_T, \quad (7)$$

where we have written the dimensionless form for clarity. We plot the compressibility $\tilde{\kappa} = \kappa/\kappa_0$ as a function of pressure $\tilde{p} = P/P_0$, normalized with their ideal values at zero temperature, in Fig. 4(a). From the universal function $\tilde{\kappa}(\tilde{p})$ several other thermodynamic properties of the experimental system can be found [16, 18]. Looking at Fig. 4(a), we see the compressibility for all three T -matrix theories rises above that of the ideal gas with the GG T -matrix decreasing at lower pressure. We expect the the normalized compressibility for the three T -matrix theories to lower, which in 3D marks the onset of pair formation and superfluidity [18]. However, for an interaction of $\beta\epsilon_B = 0.47$, only the fully self-consistent GG theory is reliable at low temperatures and the lowering is not seen in the GG_0 and NSR theories. We see all three theories are similar to the experimental results, with the NSR theory matching well for low pressures, and the GG theory closely matches for a wide range of values, as we would expect from the similarity found in the density and pressure equation of state for $\beta\epsilon_B = 0.47$. At low pressure the GG curve does not reach the same maximum as the experimental results and begins to lower. It is difficult to assess whether the experimental data show a similar feature due to the noise in the data; lower temperatures would be required for a further comparison.

In Fig. 4(b) we plot the scaled compressibility as a

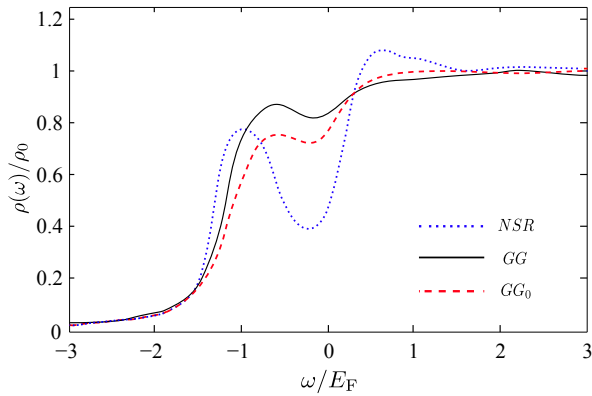


FIG. 5. (Color online) The density of states $\rho(\omega)$ is shown in units of the non-interacting density of states at the Fermi surface $\rho_0 = M/2\pi$, for $\beta\varepsilon_b = 0.47$ and $T/T_F = 0.2$ for GG (black solid), GG_0 (red dashed), and NSR (blue dotted).

function of reduced temperature. We explicitly see here for low temperatures the GG theory decreasing from a maximum value for temperatures below $T \simeq 0.2T_F$.

For the three T -matrix calculations we examine the normalized density of states, $\rho(\omega)$ and the onset of the pseudogap regime in Fig. 5 for $\beta\varepsilon_b = 0.47$ and temperature $T/T_F = 0.2$, which corresponds to an interaction strength $\eta = \ln[k_F a_{2D}] \simeq 1.5$. The density of states is computed from the spectral function $A(\mathbf{k}, \omega)$, which is found by analytically continuing the Green's function to real frequencies, $A(\mathbf{k}, \omega) = \text{Im} G(\mathbf{k}, \omega + i0^+)/\pi$. This is achieved through Padé approximants [31] and the density of states then follows as the momentum average of the spectral function $\rho(\omega) = \int d\mathbf{k} A(\mathbf{k}, \omega)/(2\pi)^2$. There are two methods used to calculate the density of states, analytically continuing the self-energy or the Green's function directly. Using the self-energy produces a smoother density of states as the numerical integration of the spectral function is considerably simpler. This method is used for the calculation used in the GG and GG_0 theory and the Green's function is directly continued for the NSR theory.

The interaction and temperature used in the calculation of $\rho(\omega)$ in Fig. 5 are experimentally attainable. At $T/T_F = 0.2$ and $\beta\varepsilon_b = 0.47$ the converged chemical potential μ for each of the T -matrix theories is larger than zero, and for the GG theory the compressibility is low-

ering. We see that for each of the T -matrix theories the density of states at the chemical potential becomes suppressed, and at either side we see an increase in the density of states, indicative of a pseudogap. There is no precise definition for the onset of the pseudogap; it is, however, most likely too small an effect in the GG and GG_0 theories at this temperature and interaction strength for us to confidently say that there is indeed a pseudogap, however, at lower temperatures and larger interactions, the effect becomes more pronounced [5]. Looking at the NSR theory there is a significant increase of the density of states and there is a pseudogap phase at this temperature and interaction. Thus, we would expect for an interaction strength of $\beta\varepsilon_b \simeq 0.47$ and temperatures lower than $T/T_F \simeq 0.2$ that the system would contain a pseudogap regime.

In conclusion, we have compared three T -matrix theories with experiment and found in the normal phase the fully-self consistent GG T -matrix theory agrees well with a wide range of temperatures and interactions. Comparatively, the GG_0 and NSR T -matrix schemes underestimate the density and pressure equation of state in the strongly interacting regime. Examining the density of states, we have shown that each theory predicts a pseudogap at a temperature and interaction strength accessible in current experiments. Comparing the universal function $\tilde{\kappa}(\tilde{p})$ found from experiment and the T -matrix theories, we see a difference at low temperature close to the BKT transition. In order to understand the below T_c thermodynamic properties, a theory beyond the T -matrix approximations must be used where we can explicitly take into account the superfluidity.

Note added: Recently, we became aware of a related paper [32] that examines the thermodynamics of a 2D Fermi gas across the BCS-BEC crossover. This work found similar results but focused on the BEC side of the crossover.

ACKNOWLEDGMENTS

We would like to thank Giacomo Bighin and Luca Salasnich us for giving their data, Meera Parish for useful discussions, and the ARC Discovery Projects (FT130100815, DP140100637, DP140103231 and FT140100003).

-
- [1] P. A. Lee, N. Nagaosa, and X.-G. Wen, *Rev. Mod. Phys.* **78**, 17 (2006).
 - [2] V. M. Loktev, R. M. Quick, and S. G. Sharapov, *Physics Reports* **349**, 1 (2001).
 - [3] J. Levinsen and M. M. Parish, in *Annual Review of Cold Atoms and Molecules*, Vol. 3 (World Scientific, Singapore, 2015) pp. 1–75.
 - [4] R. Haussmann, *Z. Phys. B: Condens. Mat.*, **91**, 291 (1993).

- [5] M. Bauer, M. M. Parish, and T. Enss, *Phys. Rev. Lett.* **112**, 135302 (2014).
- [6] F. Marsiglio, P. Pieri, A. Perali, F. Palestini, and G. C. Strinati, *Phys. Rev. B* **91**, 054509 (2015); V. Pietilä, *Phys. Rev. A* **86**, 023608 (2012); R. Watanabe, S. Tsuchiya, and Y. Ohashi, *Phys. Rev. A* **88**, 013637 (2013).
- [7] H. Hu, P. D. Drummond, and X.-J. Liu, *Nat Phys* **3**, 469 (2007); H. Hu, X.-J. Liu, and P. D. Drummond,

- New Journal of Physics **12**, 063038 (2010); S. Tsuchiya, R. Watanabe, and Y. Ohashi, Phys. Rev. A **80**, 033613 (2009).
- [8] G. Bertaina and S. Giorgini, Phys. Rev. Lett. **106**, 110403 (2011).
- [9] H. Shi, S. Chiesa, and S. Zhang, Phys. Rev. A **92**, 033603 (2015).
- [10] E. R. Anderson and J. E. Drut, Phys. Rev. Lett. **115**, 115301 (2015).
- [11] J. Vlietinck, J. Ryckebusch, and K. Van Houcke, Phys. Rev. B **89**, 085119 (2014).
- [12] X.-J. Liu, H. Hu, and P. D. Drummond, Phys. Rev. B **82**, 054524 (2010).
- [13] M. Barth and J. Hofmann, Phys. Rev. A **89**, 013614 (2014); V. Ngampruetikorn, J. Levinsen, and M. M. Parish, Phys. Rev. Lett. **111**, 265301 (2013).
- [14] P. Dyke, K. Fenech, T. Peppler, M. G. Lingham, S. Hoinka, W. Zhang, B. Mulkerin, H. Hu, X.-J. Liu, and C. J. Vale, (2014), arXiv:1411.4703.
- [15] P. A. Murthy, D. Kedar, T. Lompe, M. Neidig, M. G. Ries, A. N. Wenz, G. Zürn, and S. Jochim, Phys. Rev. A **90**, 043611 (2014).
- [16] K. Fenech, P. Dyke, T. Peppler, M. G. Lingham, S. Hoinka, H. Hu, and C. J. Vale, (2015), arXiv:1508.04502.
- [17] M. G. Ries, A. N. Wenz, G. Zürn, L. Bayha, I. Boettcher, D. Kedar, P. A. Murthy, M. Neidig, T. Lompe, and S. Jochim, Phys. Rev. Lett. **114**, 230401 (2015); P. A. Murthy, I. Boettcher, L. Bayha, M. Holzmann, D. Kedar, M. Neidig, M. G. Ries, A. N. Wenz, G. Zürn, and S. Jochim, Phys. Rev. Lett. **115**, 010401 (2015).
- [18] M. J. H. Ku, A. T. Sommer, L. W. Cheuk, and M. W. Zwierlein, Science **335**, 563 (2012).
- [19] B. Fröhlich, M. Feld, E. Vogt, M. Koschorreck, W. Zwerger, and M. Köhl, Phys. Rev. Lett. **106**, 105301 (2011); M. Feld, B. Fröhlich, E. Vogt, M. Koschorreck, and M. Köhl, Nature (London) **480**, 75 (2011).
- [20] A. Perali, F. Palestini, P. Pieri, G. C. Strinati, J. T. Stewart, J. P. Gaebler, T. E. Drake, and D. S. Jin, Phys. Rev. Lett. **106**, 060402 (2011); J. P. Gaebler, J. T. Stewart, T. E. Drake, D. S. Jin, A. Perali, P. Pieri, and G. C. Strinati, Nat Phys **6**, 569 (2010); J. T. Stewart, J. P. Gaebler, and D. S. Jin, Nature (London) **454**, 744 (2008).
- [21] H. Hu, X.-J. Liu, and P. D. Drummond, Phys. Rev. A **77**, 061605 (2008).
- [22] R. Haussmann, M. Punk, and W. Zwerger, Phys. Rev. A **80**, 063612 (2009); C.-C. Chien, H. Guo, Y. He, and K. Levin, Phys. Rev. A **81**, 023622 (2010).
- [23] R. Haussmann, Phys. Rev. B **49**, 12975 (1994).
- [24] S. K. Adhikari, American Journal of Physics **54**, 362 (1986).
- [25] P. Nozières and S. Schmitt-Rink, Journal of Low Temperature Physics **59**, 195 (1985).
- [26] M. Randeria, J.-M. Duan, and L.-Y. Shieh, Phys. Rev. Lett. **62**, 981 (1989); Phys. Rev. B **41**, 327 (1990); J. R. Engelbrecht and M. Randeria, Phys. Rev. Lett. **65**, 1032 (1990); S. Schmitt-Rink, C. M. Varma, and A. E. Ruckenstein, Phys. Rev. Lett. **63**, 445 (1989).
- [27] J. W. Serene, Phys. Rev. B **40**, 10873 (1989).
- [28] L. He, H. Lü, G. Cao, H. Hu, and X.-J. Liu, Phys. Rev. A **92**, 023620 (2015).
- [29] R. Desbuquois, T. Yefsah, L. Chomaz, C. Weitenberg, L. Corman, S. Nascimbène, and J. Dalibard, Phys. Rev. Lett. **113**, 020404 (2014).
- [30] G. Bighin and L. Salasnich, (2015), arXiv:1507.07542.
- [31] K. S. D. Beach, R. J. Gooding, and F. Marsiglio, Phys. Rev. B **61**, 5147 (2000).
- [32] I. Boettcher, L. Bayha, D. Kedar, P. A. Murthy, M. Neidig, M. G. Ries, A. N. Wenz, G. Zürn, S. Jochim, and T. Enss, (2015), arXiv:1509.03610.